

## Fine Structure in the Decay of the Highly Deformed Proton Emitter $^{131}\text{Eu}$

A. A. Sonzogni,<sup>1</sup> C. N. Davids,<sup>1</sup> P. J. Woods,<sup>2</sup> D. Seweryniak,<sup>1,3</sup> M. P. Carpenter,<sup>1</sup> J. J. Ressler,<sup>3</sup> J. Schwartz,<sup>1,4</sup>  
J. Uusitalo,<sup>1</sup> and W. B. Walters<sup>3</sup>

<sup>1</sup>Physics Division, Argonne National Laboratory, Argonne, Illinois 60439

<sup>2</sup>University of Edinburgh, Edinburgh, EH9 3JZ, United Kingdom

<sup>3</sup>Department of Chemistry, University of Maryland, College Park, Maryland 20742

<sup>4</sup>Department of Physics, Yale University, New Haven, Connecticut 06511

(Received 12 May 1999)

Fine structure in the ground-state proton radioactive decay of highly deformed  $^{131}\text{Eu}$  has been identified. In addition to the previously observed ground-state line, measured here with a proton energy of 932(7) keV, a second proton peak with energy 811(7) keV was observed. We interpret this line as proton decay from the  $^{131}\text{Eu}$  ground state to the first excited  $2^+$  state of the daughter nucleus  $^{130}\text{Sm}$ . Comparing the measured branching ratio with calculations enables the ground-state configuration of  $^{131}\text{Eu}$  to be unambiguously assigned to the  $3/2^+[411]$  Nilsson configuration.

PACS numbers: 23.50.+z, 21.10.Re, 21.10.Tg, 27.60.+j

Ground-state proton radioactivity is a phenomenon associated with heavy nuclei lying beyond the proton drip-line [1]. Proton decay rates are extremely sensitive to the orbital angular momentum of the proton,  $\ell_p$ , and can be used to characterize nuclear configurations at the extreme limit of stability. For spherical nuclei  $\ell_p$  is a good quantum number and the proton decay spectroscopic factors are in general well reproduced by calculations [2,3]. Long-standing exceptions to this rule are the proton decays of  $^{109}\text{I}$  and  $^{113}\text{Cs}$  [4] which can be reproduced only by using a deformed multiparticle calculational approach [5,6] with a quadrupole deformation  $\beta_2 \sim 0.1$ .

In a recent Letter, we reported on the discovery of proton radioactivity from the highly deformed ( $\beta_2 \sim 0.3$ ) nuclei  $^{131}\text{Eu}$  and  $^{141}\text{Ho}$  [7]. The half-lives of these nuclei could not be reproduced using a spherical basis, whereas deformed calculations of the type developed in [5,6] could reproduce the decay rates [7]. The results were consistent with Nilsson configurations and deformations predicted by macroscopic-microscopic calculations [8,9]. These indicate that there is a rapid change to high prolate deformations in the region of the proton drip-line below  $Z = 69$  which reaches its apogee around  $^{131}\text{Eu}$ . Highly deformed nuclei are a natural region to search for the new phenomenon of proton decay fine structure, since low-lying first excited  $2^+$  states in the daughter nuclei may receive significant decay strength relative to the ground state. The decay rate to the  $2^+$  daughter state will be sensitive to different components of the parent wave function. The present Letter describes the discovery of fine structure in the proton-radioactive decay of  $^{131}\text{Eu}$ , and presents the first nuclear structure information on the daughter nucleus  $^{130}\text{Sm}$ .

A 2 pA beam of 402 MeV  $^{78}\text{Kr}$  ions produced by the ATLAS accelerator facility was used to bombard a  $0.77\text{ mg/cm}^2$  thick  $^{58}\text{Ni}$  target resulting in a compound nucleus excitation energy of  $\sim 82$  MeV at the center of

the target, chosen to optimize production of  $^{131}\text{Eu}$  nuclei. The Argonne Fragment Mass Analyzer [10] was set to analyze  $A = 131$  ions with charge states  $q = 32$  and  $33$ , with slits being placed at the focal plane to allow only the transmission of these ions into a  $60\text{-}\mu\text{m}$ -thick double-sided silicon strip detector (DSSD) system, previously described in Ref. [2].

A  $4.6\text{ mg/cm}^2$  thick Ni foil was available 8 cm in front of the DSSD to degrade the energies of recoiling  $^{131}\text{Eu}$  ions and thereby to control their implantation depth into the DSSD. The experiment was run for approximately two days without this foil in place, resulting in an implantation depth of  $\sim 20\text{ }\mu\text{m}$ , greater than the  $\sim 15\text{ }\mu\text{m}$  range of the  $^{131}\text{Eu}$  protons. Decays occurring within 100 ms of an  $A = 131$  ion implanted into the same DSSD quaspixel are displayed in Fig. 1(a). The small amount of background in Fig. 1(a) is produced by  $\beta$ -delayed protons from the decay of more intensely produced isobars. This background was partially vetoed by rejecting DSSD events appearing in coincidence with protons measured in a box of Si strip detectors surrounding the front side of the DSSD or in a large area Si detector placed behind the DSSD. Two peaks can be seen in Fig. 1(a) (with an estimated combined production cross section of  $\sim 70$  nb), the one at higher energy corresponding to the previously identified  $^{131}\text{Eu}$  ground state-to-ground state proton transition [ $E_p = 932(7)$  keV,  $t_{1/2} = 17.8(19)$  ms], and the lower one having  $E_p = 811(7)$  keV,  $t_{1/2} = 23_{-6}^{+10}$  ms, both calibrated with respect to the 1064(6) keV proton from the decay of  $^{167}\text{Ir}^m$  [2]. The energy of the ground-state group measured in the present experiment is slightly lower than the value of 950(8) keV obtained in Ref. [7]. For the purposes of the calculations discussed below, the energy measured in the present work will be used.

The fact that two proton groups separated in energy by 121(3) keV have half-lives in agreement with one another suggests that the low energy group also originates from

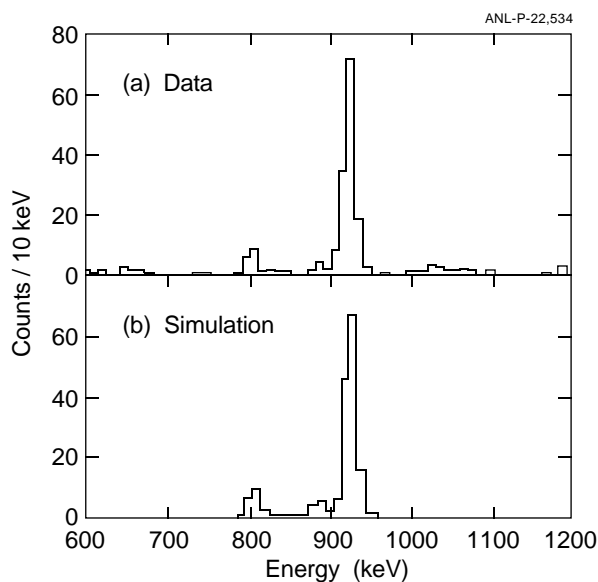


FIG. 1. (a) Observed energy spectrum of protons from the decay of  $^{131}\text{Eu}$ , obtained under the gating conditions given in the text. (b) Simulated energy spectrum of protons from the decay of  $^{131}\text{Eu}$ , assuming an implantation depth of  $19.3 \mu\text{m}$ , a  $2^+$  excitation energy in  $^{130}\text{Sm}$  of  $122 \text{ keV}$  and a  $2^+$  decay branching ratio of  $0.24(5)$  (see text for details).

the decay of the  $^{131}\text{Eu}$  ground state. This represents the first example of proton decay fine structure. Nothing is known experimentally about the levels of the daughter nucleus  $^{130}\text{Sm}$ . On the basis of systematics, it is most likely that the excited daughter state has a spin parity of  $2^+$ . We shall demonstrate in the following discussions that such an interpretation is in excellent agreement with proton decay and shape prediction calculations.

After being populated by proton decay, the  $2^+$  state can decay to the ground state either by gamma-ray emission or internal conversion. In the latter case, the detected energy signals of the proton and the electron will sum, thus removing counts from the  $2^+$  proton peak. To correct the yield of the  $2^+$  proton peak, a Monte Carlo simulation of the energy spectrum in the DSSD for proton decays was performed. The calculation started with the implantation of the  $^{131}\text{Eu}$  atom in the Si detector, followed by the proton emission, and the subsequent gamma or electron emission if the  $2^+$  state was populated. Input values for the simulation were the implantation depth of the  $^{131}\text{Eu}$  atom, the energy of the ground state-to-ground state decay proton, the thickness of the DSSD, the energy of the  $2^+$  state, the internal conversion coefficient of the  $2^+ \rightarrow 0^+$  transition, and the experimental proton energy resolution. The measured excitation energy of the  $2^+$  state in  $^{130}\text{Sm}$  is  $122(3) \text{ keV}$ , leading to a total internal conversion coefficient  $\alpha_T$  of  $1.16$  [11]. Most of the data were taken with  $^{131}\text{Eu}$  kinetic energies of  $170 \text{ MeV}$ , which translates into an implantation depth of  $19.3 \mu\text{m}$ . A small fraction of the data was taken with a  $4.6 \text{ mg/cm}^2$

Ni degrader foil in front of the DSSD, which decreased the energy of the  $^{131}\text{Eu}$  ions down to  $23 \text{ MeV}$ . In this case, the implantation depth was  $5.3 \mu\text{m}$ , and these data showed the two proton peaks to be present, ruling out any anomalous implantation depth/recoil energy effects for the observed fine structure. The branching ratio for decay to the  $2^+$  state,  $\Gamma_{2^+}/[\Gamma_{2^+} + \Gamma_{0^+}]$ , where the  $\Gamma_i$ 's are the appropriate partial decay widths, was used as a parameter, and the value obtained from the simulations after the resulting spectrum agreed with the experimental energy spectrum was  $0.24(5)$ .

The simulated spectrum for the deep implantation case is shown in Fig. 1(b). Good agreement with the data [Fig. 1(a)] is observed. The small peak between the  $2^+$  and ground-state peaks corresponds to the sum of  $K$  electrons and  $811 \text{ keV}$  protons.

The branching ratios for decay to the  $2^+$  state have been calculated using the deformed formalism of Ref. [7]. This formalism has been extended to cover the case of decay to states in the daughter nucleus having final spin  $J_f > 0$ . This allows more than one angular momentum combination ( $j_p \ell_p$ ) for the outgoing proton to be involved in the decay process, and opens up the possibility of probing different components of the parent nucleus wave function. For proton decay from the initial state  $J_i K_i$  feeding the ground state, the decay width is given by

$$\Gamma_{0^+} = \Gamma_{J_f=0^+}^{J_i K_i, j_p \ell_p}.$$

Here  $\Gamma_{J_f j_p \ell_p}^{J_i K_i} = 2\pi |B|^2$ , where  $B$  is the distorted wave Born approximation transition amplitude given in Ref. [7]. For protons feeding the  $2^+$  state,

$$\Gamma_{2^+} = \sum_{j_p \ell_p} \Gamma_{J_f=2^+}^{J_i K_i, j_p \ell_p}.$$

The total decay width is

$$\Gamma = \Gamma_{0^+} + \Gamma_{2^+}.$$

For the cases considered here ( $J_i^\pi = 3/2^+$  or  $5/2^+$ ), the permissible angular momentum combinations ( $j_p \ell_p$ ) for the outgoing proton are subject to the conditions  $\vec{J}_i = \vec{J}_f + \vec{j}_p$  and  $\ell_p$  even. Figure 2 shows the results of the branching ratio calculations, plotted for a range of high quadrupole deformations. As in Ref. [7], we have neglected the effect of pairing in the daughter nucleus and possible small shape differences between parent and daughter nuclei. The curves represent branching ratios from the two candidate  $^{131}\text{Eu}$  ground-state Nilsson orbitals,  $3/2^+[411]$  and  $5/2^+[413]$ . While the ground state-to-ground state decay data alone were not sufficient to decide between the two possibilities [7], it is clear from Fig. 2 that the fine structure data are able to unambiguously show that the correct Nilsson orbital

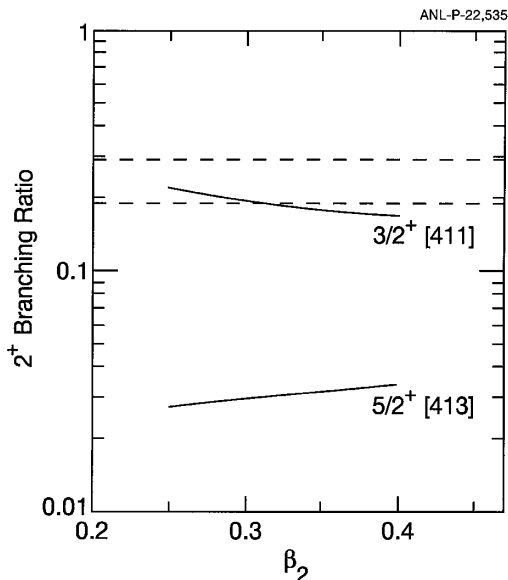


FIG. 2. Calculated  $2^+$  decay branching ratios for  $^{131}\text{Eu}$  as a function of the quadrupole deformation parameter  $\beta_2$ , based on the  $3/2^+[411]$  and  $5/2^+[413]$  Nilsson orbitals. The observed branching ratio lies in the band between the dashed lines.

assignment for the  $^{131}\text{Eu}$  ground state is  $3/2^+[411]$ , as predicted by Möller *et al.* [9], and at variance with the recent proposed assignment of  $K = 5/2^+$  by Maglione *et al.* [12].

The calculations show that for the  $3/2^+[411]$  configuration, the ground-state partial decay width  $\Gamma_{0^+}$  receives most of its strength from the  $d_{3/2}$  and  $d_{5/2}$  components of the parent wave function, which contribute in the ratio of about 1.6:1. The  $2^+$  decay width  $\Gamma_{2^+}$  receives 95% of its strength from the  $d_{5/2}$  component of the  $^{131}\text{Eu}$  ground state wave function. For the  $5/2^+[413]$  configuration, the predicted branching ratio is much smaller. This is because the largest contribution to  $\Gamma_{2^+}$  comes from the  $\ell_p = 2$   $d_{5/2}$  component of the wave function, which comprises only 1% of the wave function. The remainder is made up of the  $\ell_p = 4$   $g_{7/2}$  and  $g_{9/2}$  terms.

Applying the Grodzins formula [13,14] to the  $2^+$  excitation energy of 122 keV yields a quadrupole deformation  $\beta_2 = 0.34$  for  $^{130}\text{Sm}$ . This gives direct confirmation of the conclusions of Ref. [7] that a region of high prolate deformation develops below  $Z = 69$  along the region of the proton drip-line. This value compares very well with the value of  $\beta_2 = 0.33$  predicted by the macroscopic-microscopic model of Möller *et al.* [8] for  $^{130}\text{Sm}$ . The corresponding prediction for the proton-emitting ground state of  $^{131}\text{Eu}$  is  $\beta_2 = 0.33$  [8], implying that the deformed core is essentially inert during the proton decay process, an assumption used in the present calculations.

The total half-life for  $^{131}\text{Eu}$  is measured here to be 17.8(19) ms. Assuming a  $\beta$ -decay partial half-life of 147 ms [9] we have used the calculational methods of Ref. [7] and  $\beta_2 = 0.34$  to obtain proton partial half-lives of 27.9 and 128 ms for the ground- and excited-state transitions, respectively. These agree well with the experimental values of 26.6(37) and 84(20) ms.

In summary, proton decay fine structure is reported here for the first time. The observation of a second proton decay branch for the  $^{131}\text{Eu}$  ground state has allowed different components of its wave function to be probed, and has identified its Nilsson configuration as the  $3/2^+[411]$  orbital. These new data also provide a direct insight into the large ground-state deformations in this region of the proton drip-line. Proton decay rate calculations using such a high deformation value are able to reproduce well the measured partial proton half-lives, providing detailed insight into the role of deformation in this quantum tunneling phenomenon.

The authors wish to thank S. Kadmsky for valuable discussions, and P. Butler for the use of his Monte Carlo code Ritupad. P.J.W. wishes to acknowledge travel support from NATO under Grant No. CRG 940303. This work was supported by the U.S. Department of Energy, Nuclear Physics Division, under Contract No. W-31-109-ENG-38 (Argonne National Laboratory) and Grant No. DE-FG02-94ER40834 (University of Maryland).

- [1] P.J. Woods and C.N. Davids, *Annu. Rev. Nucl. Part. Sci.* **47**, 541 (1997).
- [2] C.N. Davids *et al.*, *Phys. Rev. C* **55**, 2255 (1997).
- [3] S. Åberg, P.B. Semmes, and W. Nazarewicz, *Phys. Rev. C* **56**, 1762 (1997); **58**, 3011 (1998).
- [4] A. Gillitzer *et al.*, *Z. Phys. A* **326**, 107 (1987).
- [5] V.P. Bugrov and S.G. Kadmsky, *Sov. J. Nucl. Phys.* **49**, 967 (1989).
- [6] S.G. Kadmsky and V.P. Bugrov, *Phys. At. Nucl.* **59**, 399 (1996).
- [7] C.N. Davids *et al.*, *Phys. Rev. Lett.* **80**, 1849 (1998).
- [8] P. Möller, J.R. Nix, W.D. Myers, and W.J. Swiatecki, *At. Data Nucl. Data Tables* **59**, 185 (1995).
- [9] P. Möller, J.R. Nix, and K.-L. Kratz, *At. Data Nucl. Data Tables* **66**, 131 (1997).
- [10] C.N. Davids *et al.*, *Nucl. Instrum. Methods Phys. Res., Sect. B* **70**, 358 (1992).
- [11] F. Rösel, H.M. Fries, K. Alder, and H.C. Pauli, *At. Data Nucl. Data Tables* **21**, 91 (1978).
- [12] E. Maglione, L.S. Ferreira, and R.J. Liotta, *Phys. Rev. C* **59**, R589 (1999).
- [13] L. Grodzins, *Phys. Lett.* **2**, 88 (1962).
- [14] F.S. Stephens *et al.*, *Phys. Rev. Lett.* **29**, 438 (1972).